Observational Study

Medicine®

OPEN

# Higher subcortical and white matter cerebral blood flow in perinatally HIV-infected children

Charlotte Blokhuis, MD[a,*], Henri J.M.M. Mutsaerts, MD, PhD[b,c], Sophie Cohen, MD, PhD[a], Henriëtte J. Scherpbier, MD, PhD[a], Matthan W.A. Caan, PhD[b], Charles B.L.M. Majoie, MD, PhD[b], Taco W. Kuijpers, MD, PhD[a], Peter Reiss, MD, PhD[d,e,f], Ferdinand W.N.M. Wit, MD, PhD[d,e,f], Dasja Pajkrt, MD, PhD[a]

**Abstract**

This study aimed to evaluate cerebral blood flow (CBF) in pediatric human immunodeficiency virus (HIV)-infection, and its role in HIV-related cerebral injury and cognitive impairment.

This cross-sectional observational study compared 28 perinatally HIV-infected children (8–18 years) to 34 healthy controls matched for age, sex, ethnicity, and socio-economic status. All participants underwent 3-Tesla magnetic resonance imaging, using arterial spin labeling to assess CBF in gray matter (GM), white matter (WM), basal ganglia, and thalamus. We used linear regression analysis to evaluate group differences and associations with HIV disease and treatment characteristics, macrostructural (volume loss, WM lesions) or microstructural injury (increased WM diffusivity, neurometabolite alterations), or poorer cognitive performance.

HIV-infected children had higher CBF in WM (+10.2%; $P=0.042$), caudate nucleus (+4.8%; $P=0.002$), putamen (+3.6%; $P=0.017$), nucleus accumbens (+3.9%; $P=0.031$), and thalamus (+5.5%; $P=0.032$). Thalamus CBF was highest in children with a Centers for Disease Control and Prevention stage B (Coef. = 6.45; $P=0.005$) or C (Coef. = 8.52; $P=0.001$) diagnosis. Lower GM CBF was associated with higher WM lesion volume in HIV-infected children (Coef. = −0.053; $P=0.001$). No further associations with HIV-related cognitive impairment or cerebral injury were found.

CBF was higher in WM, basal ganglia, and thalamus in combination antiretroviral therapy (cART)-treated perinatally HIV-infected children, but this was not associated with cerebral injury or cognitive impairment. HIV-infected children with lower GM CBF had a higher volume of WM lesions, which could reflect vascular disease as potential contributing factor to white matter injury. Lifelong exposure to HIV and cART in this population warrants longitudinal assessment of CBF and how it relates to (neuro)inflammation, vascular dysfunction, and cerebral injury in pediatric HIV.

**Abbreviations:** AD = axial diffusivity, AMC = Academic Medical Center, ASL = arterial spin labeling, cART = combination antiretroviral therapy, CBF = cerebral blood flow, GM = gray matter, HIV = human immunodeficiency virus, Ht = hematocrit, ICV = intracranial volume, IQ = intellinge quotient, MRI = magnetic resonance imaging, MRS = magnetic resonance spectroscopy, PET = positron emission tomography, ROI = region of interest, VL = viral load, WM = white matter, WML = white matter lesions.

**Keywords:** adolescent, cerebrovascular circulation, child, cognitive function, HIV, magnetic resonance imaging

*Editor: Kirsty Donald.*

*CB (Department of Pediatric Hematology, Immunology and Infectious Diseases) takes full responsibility for the data analyses and interpretation, had full access to all of the data, and the right to publish any and all data separate and apart from any sponsor.*

*CB analyzed the data including statistical analysis, interpreted the results, and drafted the manuscript. HJMMM performed MRI postprocessing, interpreted the results, and revised the manuscript. SC recruited patients and controls, coordinated study visits, performed MRI scans, and revised the manuscript. HJS recruited patients, supervised study design, and revised the manuscript. MWAC designed the study, conceptualized the imaging protocol, supervised MRI scanning, and revised the manuscript. CBLMM conceptualized the imaging protocol, supervised MRI scanning, and revised the manuscript. TWK and PR supervised study design and revised the manuscript. FWNMW advised on statistical analysis and revised the manuscript. DP designed the study, supervised study visits, interpreted results, and revised the manuscript.*

*This study was supported by the Emma foundation (grant number 11.001). This funding body had no role in the design or conduct of the study, nor in the analysis and interpretation of the results, nor the contents of the manuscript.*

*CB, HJMMM, SC, HJS, MWAC, TWK, and FWNMW report no disclosures. CBLMM's institution has received lecture fees (Stryker). PR's institution has received fees for board membership (Gilead Sciences and Janssen Pharmaceutica), and research grants (Gilead Sciences, ViiV Healthcare, Janssen Pharmaceutica, Bristol Myers Squibb, and Merck). DP's institution has received research grants from Emma Foundation, AIDS Fonds, and Viiv Healthcare.*

[a] *Department of Pediatric Hematology, Immunology and Infectious Diseases, Emma Children's Hospital/Academic Medical Center, University of Amsterdam,* [b] *Department of Radiology, Academic Medical Center, University of Amsterdam, Amsterdam, The Netherlands,* [c] *Cognitive Neurology Research Unit, Sunnybrook Health Sciences Center, Toronto, Canada,* [d] *Department of Global Health, Academic Medical Center, University of Amsterdam, and Amsterdam Institute for Global Health and Development,* [e] *Department of Internal Medicine, Division of Infectious Diseases, Center for Infection and Immunity Amsterdam, Academic Medical Center,* [f] *HIV Monitoring Foundation, Amsterdam, The Netherlands.*

[*] *Correspondence: Charlotte Blokhuis, Department of Pediatric Hematology, Immunology and Infectious Diseases, Emma Children's Hospital/Academic Medical Center, University of Amsterdam, Meibergdreef 9, 1105AZ Amsterdam, The Netherlands (e-mail: c.blokhuis@amc.uva.nl).*



*Medicine (2017) 96:7(e5891)*

*Received: 23 June 2016 / Received in final form: 13 December 2016 / Accepted: 22 December 2016*

*http://dx.doi.org/10.1097/MD.0000000000005891*

## 1. Introduction

Despite treatment with combination antiretroviral therapy (cART), many children infected with human immunodeficiency virus (HIV) show cognitive impairments.[1] Increasing neuroimaging evidence implies that these impairments may be secondary to macro- and microstructural cerebral injury, including decreased gray matter (GM) volume,[2] white matter lesions (WML),[3] increased white matter (WM) diffusivity,[2,4] and neurometabolite alterations suggestive of glial proliferation.[5]

Improving our understanding of the mechanisms that contribute to cerebral injury in perinatally HIV-infected children may lead to improved monitoring and therapeutic strategies. Currently, the role of cerebral perfusion is poorly understood. Chronic pediatric HIV infection and several components of cART have been associated with vasculopathy, coagulopathy, metabolic comorbidities, and an increased risk of cerebrovascular events, all potentially influencing cerebral blood flow (CBF).[6,7] A small positron emission tomography (PET) study reported decreased cortical and increased subcortical activity in HIV-infected children without cART,[8] but no studies have evaluated CBF in cART-treated HIV-infected children.

Arterial spin labeling (ASL) noninvasively measures CBF by employing blood water as an endogenous magnetic tracer,[9] and has been successfully used to link CBF changes to cognitive performance in various pediatric populations.[10,11] In HIV-infected adults, ASL-detected regional CBF decreases in neuroasymptomatic patients, which deteriorated with increasing disease duration and cognitive deficits, suggesting that ASL-measured CBF may be a useful early biomarker of HIV-related cognitive impairment.[12]

As pediatric HIV-associated cerebral injury is widespread throughout GM, WM, and subcortical areas,[1] we hypothesized that perfusion changes may be apparent in these regions as well. Therefore, we used ASL-measured CBF to assess whether GM, WM, and subcortical perfusion differed between cART-treated, HIV-infected children, and matched healthy controls. Additionally, we explored whether increasing HIV severity was associated with CBF changes. Finally, we explored if CBF was associated with previously detected macrostructural (volume loss, WML) or microstructural injury (increased WM diffusivity, neurometabolite alterations), or poorer cognitive performance in our cohort.

## 2. Methods

The present study is part of an interdisciplinary observational cross-sectional study, evaluating neurological and neurocognitive disorders, neuroimaging, and ophthalmological alterations in perinatally HIV-1-infected children in the Netherlands (NOVICE: Neurological, cOgnitive and VIsual performance in perinatally HIV-infected ChildrEn).[13] The study adhered to the tenets of the Declaration of Helsinki and approval was obtained from the investigational review board at the Academic Medical Center (AMC) in Amsterdam. Written informed consent was obtained from all parents and from children ages 12 and above.

### 2.1. Study participants

The NOVICE study included perinatally HIV-infected children ages 8 to 18 years from the AMC Pediatric HIV Outpatient Clinic between December 2012 and January 2014. Healthy controls were recruited from similar communities in Amsterdam and group-wise matching for age, sex, ethnicity, and socioeconomic status was performed.[13] Exclusion criteria for study participation were chronic HIV-unrelated neurological disease, (history of) intracerebral neoplasms, traumatic brain injury, and psychiatric disorders. HIV parameters were obtained from the Dutch national HIV monitoring foundation (Stichting HIV Monitoring). Neuropsychological assessment was performed by a single psychologist as previously described.[13] For the present study, we included the domains that are most severely affected in pediatric HIV-infected populations: intelligence quotient (IQ), processing speed, attention/working memory, and visuomotor integration.[4,13,14]

### 2.2. Imaging

**2.2.1. Scanning protocol.** All subjects were requested to abstain from caffeine-containing beverages (≥5 h) before the magnetic resonance imaging (MRI) examination and ASL scans were performed as last MRI scan to minimize physiological CBF fluctuations. All scans were obtained using a 3.0 Tesla MRI scanner (Ingenia, Philips Healthcare, Best, The Netherlands) equipped with a 16-channel phased array head coil. The scanning protocol included a 3D T1-weighted anatomical scan for volumetric measurements and segmentation and registration purposes, 3D fluid attenuated inversion recovery for WML, diffusion tensor imaging for WM diffusivity, and magnetic resonance spectroscopy (MRS) for neurometabolites, of which the acquisition and postprocessing details have been previously described.[2,5] Perfusion-weighted/CBF scans were obtained using pseudo-continuous ASL (echo time/repetition time = 14/4000 ms, 240 × 240 $mm^2$ field of view, 20 axial 6 mm slices with 0.6 mm slicegap, resulting in $3 \times 3 \times 6.6$ $mm^3$ resolution, labeling duration = 1650 ms, postlabeling delay = 1525–2230 ms, 30 control and label pairs).

**2.2.2. Postprocessing.** Regional brain volumes were determined using the Freesurfer image analysis suite version 5.0.[2,15]

ASL postprocessing was performed with the "ExploreASL" toolbox, an in-house developed toolbox based on SPM (Statistical Parametric Mapping, Wellcome Trust Centre for Neuroimaging, London, UK).[16] We performed 3D rigid-body motion estimation, accounting for the signal intensity difference between control and label images.[17] Based on the net displacement vector,[18] motion spikes exceeding 3 standard deviations above the mean were discarded. Subjects were removed from the analysis if mean motion was more than 2 mm. The perfusion-weighted map was obtained by a pair-wise subtraction of the remaining control-label pairs, and converted to CBF values using a previously described single compartment quantification model.[19] Because hematocrit (Ht) influences the T1 relaxation rate of blood, and HIV-infected children had lower Ht in our cohort (Table 1), the mean Ht values for cases and controls were accounted for in the calculation of CBF.[20]

As CBF alterations in HIV-infected adults and children were previously reported in cortical and subcortical regions,[8,21,22] and HIV-infected children in our cohort show widespread injury throughout GM and WM,[2] we chose total GM and WM, basal ganglia (caudate nucleus, putamen, nucleus accumbens) and thalamus as our regions of interest (ROIs). GM and WM probability maps were segmented from the 3D T1-scans (Fig. 1A, B, F, G). The CBF maps were then rigid-body registered to the GM probability maps, which were nonlinearly registered to a population-based common space template (Fig. 1D and I).[23] Total GM and WM ROIs were masked with probability maps thresholded at $P > 0.8$, and the WM ROI was further slicewise

**Table 1**

**Demographic and clinical characteristics of study participants.**

| | N | HIV-infected children | N | Healthy controls | *P* |
|---|---|---|---|---|---|
| Demographics | | | | | |
| Sex: male | 28 | 15 (54) | 34 | 17 (50) | 0.88 |
| Age, y | 28 | 13.5 (11.8–15.9) | 34 | 12.0 (11.2–15.7) | 0.25 |
| Ethnicity: black | 28 | 20 (71) | 34 | 23 (68) | 0.75 |
| Hematocrit, L/L | 27 | 0.36 (0.35–0.38) | 31 | 0.39 (0.37–0.41) | 0.009* |
| HIV disease and treatment characteristics | | | | | |
| Age at diagnosis, y | 26 | 1.2 (0.5–4.5) | | | |
| CDC stage | | | | | |
| N/A | 28 | 9 (32) | | | |
| B | | 11 (39) | | | |
| C | | 8 (29) | | | |
| HIV-encephalopathy | 28 | 3 (11) | | | |
| Viral load | | | | | |
| Zenith VL, log copies/mL | 25 | 5.5 (5.1–5.9) | | | |
| Duration of undetectable VL, y | 28 | 8.7 (2.7–10) | | | |
| Undetectable blood VL | 28 | 25 (89) | | | |
| Undetectable CSF VL | 19 | 17 (89) | | | |
| $CD4^+$ T-cells | | | | | |
| Nadir $CD4^+$ T-cell count (Z-score) | 26 | −0.7 (−1.5 to −0.4) | | | |
| Lifetime duration of $CD4^+$ T-cell counts $<500 \times 10^6$/L, mo | 13† | 56.8 (16.3–94.1) | | | |
| $CD4^+$ T-cell count at inclusion (Z-score) | 28 | 0.8 (0.6–1.1) | | | |
| cART | | | | | |
| Age at cART initiation, y | 26 | 1.6 (0.9–5.3) | | | |
| cART use at study inclusion | 28 | 25 (89) | | | |
| Duration of cART treatment, y | 26 | 11.8 (7.1–14.7) | | | |
| Basal ganglia and thalamus volumes | | | | | |
| Caudate nucleus, $cm^3$ | 28 | 7.3 (6.8–7.7) | 34 | 7.1 (6.7–7.7) | 0.78 |
| Putamen, $cm^3$ | 28 | 13.9 (13.3–14.8) | 34 | 12.7 (11.5–15.1) | 0.08 |
| Nucleus accumbens, $cm^3$ | 28 | 13.9 (13.2–14.8) | 34 | 14.0 (13.2–15.0) | 0.18 |
| Thalamus, $cm^3$ | 28 | 1.5 (1.4–1.7) | 34 | 1.6 (1.4–1.8) | 0.19 |

Data are displayed as n (%) or median (interquartile range). Demographic characteristics were compared between HIV-infected participants and healthy controls using the Mann–Whitney *U* test for continuous data and Chi-squared test[2] for categorical data. Bilateral basal ganglia and thalamus volumes were compared using linear regression adjusted for age, sex, and intracranial volume.

B = moderate symptoms, C = severe symptoms or acquired immunodeficiency syndrome, cART = combination antiretroviral therapy, CDC stage = Center for Disease Control and Prevention stage, CSF = cerebrospinal fluid, HIV = human immunodeficiency virus, N/A = no/minimal symptoms, VL = HIV viral load.

† This excludes 15 children who never had CD4 T-cell counts below $<500 \times 10^6$/L.

* $P < 0.01$.

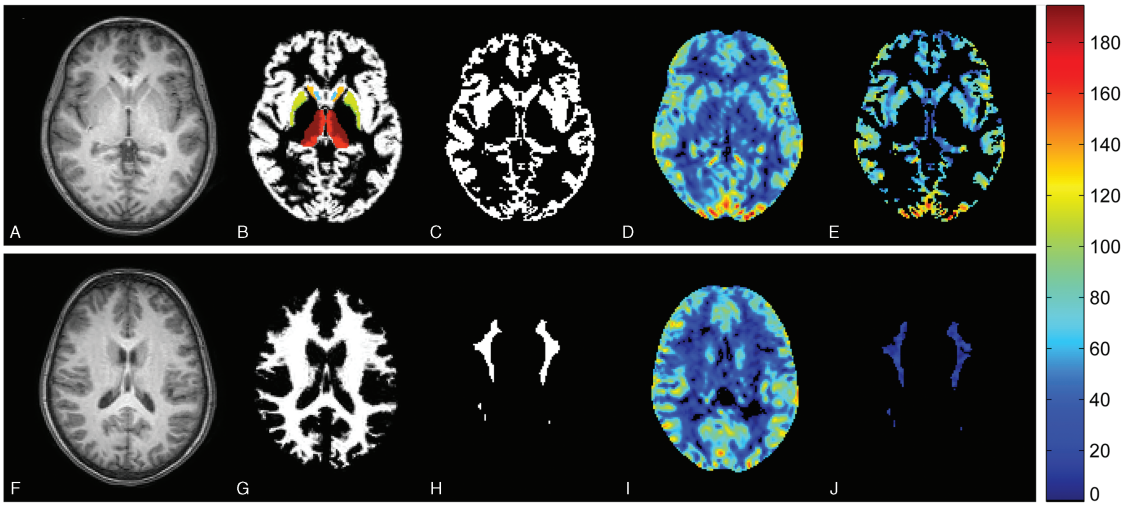


**Figure 1.** Using ASL to measure regional CBF. The panels in the first row display the process of obtaining ASL-measured CBF in GM: (A) 3D T1-scan; (B) GM probability map; (C) GM mask, obtained by WM thresholding the probability map at $P > 0.8$; (D) CBF map; (E) masked GM CBF map. The panels in the second row show the same process for WM CBF: (F) 3D T1-scan; (G) WM probability map; (H) WM mask, obtained by thresholding the WM probability map at $P > 0.8$ and eroding with a 7.5 mm disk to avoid GM contamination; (I) CBF map; (J) masked WM CBF map. The basal ganglia and thalamus regions, as defined using the Harvard Oxford atlas, are displayed in panel (B): caudate nucleus (orange), putamen (green), nucleus accumbens (blue), and thalamus (red). Note that the thalamus region contains both GM and WM, which is why it was not further masked using the participant-specific GM mask. ASL = arterial spin labeling, CBF = cerebral blood flow, GM = gray matter, WM = white matter.

eroded with a 7.5-mm radius disk to avoid GM contamination (Fig. 1B and H).[24] We defined the basal ganglia and thalamus ROIs using the Harvard-Oxford atlas (Fig. 1B), and masked the basal ganglia regions using the participant-specific GM masks.[25] We additionally corrected CBF in GM and basal ganglia for partial volume fractions.[26] As the thalamus region is composed of a mixture of GM and WM, this region was not masked by the subject-specific GM mask, nor partial volume corrected. Finally, all regional GM CBF values were normalized subject-wise using the global mean GM CBF.

### 2.3. Statistical analysis

Statistical analyses were carried out using Stata Statistical Software, release 13 (StataCorp LP, College Station, TX). We compared demographical characteristics between groups using a Mann–Whitney *U* test for continuous variables, and Chi-squared or Fisher exact test for categorical data. We compared the bilateral volumes of the caudate nucleus, putamen, nucleus accumbens, and thalamus using linear regression adjusted for age, sex, and intracranial volume (ICV). The threshold for statistical significance was set at a *P* value of 0.05.

Group differences in regional CBF and potential associations between CBF and HIV disease and treatment factors were assessed using linear regression analyses, adjusted for age above 16 years, sex, and Ht. In line with a study in healthy adolescents,[27] the relationship between CBF and age was nonlinear in our cohort, with a plateau followed by a decrease after 16 years of age. Therefore, we used the number of years of age over 16 to adjust analyses with CBF as outcome measure. To minimize potential confounding physiological effects of Ht on CBF that extend beyond its effect on T1, we additionally included Ht as a covariate in the regression models.[28] Prior to analysis, we imputed Ht if data were missing. For 1 HIV-infected participant with stable Ht measurements before and after study inclusion, we imputed Ht as determined within several weeks after study inclusion. For 3 controls, we imputed the mean Ht of the control group. Variables with a skewed distribution (zenith HIV viral load [VL], duration of CD4 T-cell count $< 500 \times 10^6$/L) were transformed using base 10 log to approach a normal distribution, and CD4 T-cell counts were transformed to age-specific Z-scores.

We then assessed whether CBF was associated with any of the MRI[2–5] or neurocognitive[4,13,14] outcomes previously shown to be affected in HIV-infected children. We included volumetric measurements and WML as markers of macrostructural cerebral injury, WM diffusivity and MRS neurometabolites as markers of microstructural injury, and IQ, processing speed, attention/working memory, and visuomotor integration to indicate cognitive performance. We explored associations between CBF and these outcomes using linear regression analyses adjusted for age (full range), sex, and Ht, and additionally for ICV if the outcome was a volumetric measurement.

## 3. Results

### 3.1. Study participants

Of the 35 HIV-infected children and 37 healthy controls originally included in the NOVICE cohort, 5 HIV-infected children did not complete MRI scanning due to dental braces (n = 2), claustrophobia (n = 1), lack of parental consent for the scan (n = 1), and early interruption of the scan due to headache (n = 1). Additionally, ASL-acquired data from 1 HIV-infected participant and 3 healthy controls were excluded due to motion artifacts (n = 2) and labeling artifacts (n = 2). Demographical and clinical data of 28 HIV-infected children (median age 13.5; 54% male, 71% black) and 34 healthy age, sex, and ethnicity-matched controls (median age 12.0; 50% male; 68% black) are summarized in Table 1. HIV-infected children were diagnosed at a median age of 1.2 years, and 8 children (29%) had a CDC stage C diagnosis at that time. At study inclusion, 89% of the HIV-infected children were using cART and had undetectable plasma HIV VL. We detected no difference in basal ganglia volumes in HIV-infected children and controls; other MRI outcomes were previously published.[2,5]

**Table 2**

**CBF in HIV-infected children and healthy controls.**

| CBF | HIV-infected children (n = 28) | Healthy controls (n = 34) | *P* |
|---|---|---|---|
| Gray matter | 65.8 (10.5) | 64.8 (9.4) | 0.72 |
| White matter | 14.0 (3.2) | 12.7 (2.3) | 0.042* |
| Caudate nucleus | 59.3 (4.2) | 56.6 (4.9) | 0.002** |
| Putamen | 57.3 (4.5) | 55.3 (5.3) | 0.017* |
| Thalamus | 46.3 (6.1) | 43.9 (5.3) | 0.032* |
| Nucleus accumbens | 55.8 (5.9) | 53.7 (8.5) | 0.031* |

Results of the age-, sex-, and hematocrit (Ht)-corrected regression analysis comparing ASL-measured CBF between HIV-infected children and healthy controls. CBF was calculated with corrections for the effect of Ht on blood T1 and for partial volume fractions. Subcortical CBF values were normalized subject-wise using the overall mean gray matter CBF. Data are displayed as mean (standard deviation).
ASL = arterial spin labeling, CBF = cerebral blood flow, HIV = human immunodeficiency virus.
* $P < 0.05$.
** $P < 0.01$.

### 3.2. CBF in HIV-infected children and healthy controls

Results of the ROI-based regression analyses comparing CBF between HIV-infected children and controls are shown in Table 2 and Fig. 2. HIV-infected children had higher CBF in WM (+10.2%; $P = 0.042$) and basal ganglia, including the caudate nucleus (+4.8%; $P = 0.002$), putamen (+3.6%; $P = 0.017$), nucleus accumbens (+3.9%; $P = 0.031$), and thalamus (+5.5%; $P = 0.032$). GM CBF did not differ significantly between groups.

Table 3 shows that children with a history of a CDC stage B or C diagnosis had higher thalamus CBF as compared to those diagnosed with CDC stage N/A (stage B: Coef. = 6.45, $P = 0.005$; stage C: Coef. = 8.52, $P = 0.001$). A longer duration of viral suppression was associated with lower caudate nucleus CBF (Coef. = −0.510, $P = 0.009$). A higher peak HIV VL was associated with higher GM CBF (Coef. = 7.61, $P = 0.025$) but lower caudate nucleus CBF (Coef. = −2.66, $P = 0.041$). Longer immune suppression, reflected in a longer lifetime duration of $CD4^+$ T-cell count $< 500 \times 10^6$/L, was associated with lower nucleus accumbens CBF (Coef. = −10.06, $P = 0.027$).

Associations between CBF and macrostructural MRI biomarkers are shown in Table 4. In HIV-infected children, lower GM CBF was associated with higher WML volume (Coef. = −0.05, $P = 0.039$), and showed a trend toward association with presence of WML (Coef. = −0.26, $P = 0.054$). CBF was not associated with cerebral volume in HIV-infected children, whereas in healthy controls, caudate nucleus CBF and volume were associated (Coef. = 0.091, $P = 0.012$).

CBF was not associated with increased WM diffusivity or altered neurometabolites in HIV-infected children (Table 5). In healthy controls, higher GM CBF was associated with a higher axial diffusivity (AD; Coef. = 0.10, $P = 0.015$), indicating better axonal health.

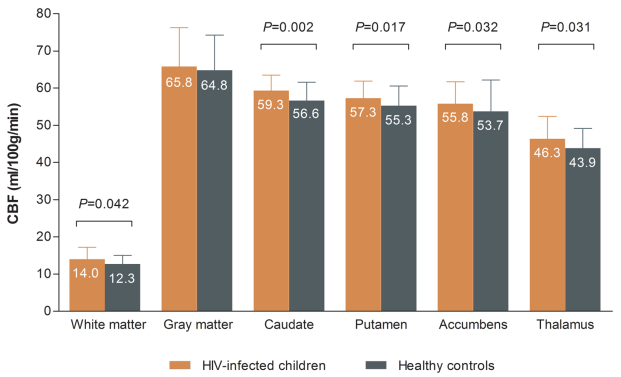


**Figure 2.** HIV-infected children have higher CBF in white matter, basal ganglia, and thalamus. We compared ASL-measured CBF between HIV-infected children and healthy controls using linear regression analysis adjusted for age (>16 years), sex, and hematocrit. Prior to analysis, CBF values for caudate nucleus, putamen, nucleus accumbens, and thalamus were normalized subject-wise using the overall mean gray matter CBF. The error bars represent standard deviations. ASL = arterial spin labeling, CBF = cerebral blood flow, HIV = human immunodeficiency virus.

No associations were found between CBF and cognitive performance in HIV-infected children (Table 6). In healthy controls, higher GM CBF was associated with attention/working memory performance (Coef. = 0.11, $P = 0.029$).

## 4. Discussion

Our study suggests that cART-treated, perinatally HIV-infected children have higher CBF in WM, basal ganglia, and thalamus as compared to matched healthy controls. A more severe HIV disease history did not consistently predict more pronounced CBF changes. The association between lower GM CBF and WML volume in HIV-infected children proposes a potential vascular contribution to the etiology of these lesions. Otherwise, our findings indicate no direct associations between CBF and previously detected HIV-related MRI abnormalities or cognitive impairment. Apparently, the cerebral perfusion differences found in cART-treated, HIV-infected children do not directly translate to current brain pathology and clinical phenotype. However, it may reflect stable or cumulative damage originating from uncontrolled disease early in life.

Basal ganglia hypermetabolism was previously detected in children with HIV-encephalopathy[8] as well as in cART-treated adults with mild psychomotor symptoms.[29] Conversely, PET and ASL studies in more severe neurosymptomatic HIV-infected adults have reported basal ganglia hypometabolism and CBF decreases.[12,29] This has led to the proposal of a biphasic disease process affecting the basal ganglia in adults. The first, acute phase is characterized by increased CBF and concentrations of choline and myo-inositol,[29,30] indicative of glial proliferation, and the second, chronic phase is clinically marked by more severe psychomotor decline, along with decreased CBF,[29] volume loss,[12] and lower N-acetylaspartate concentrations,[30] likely due to cell death. In our study, however, we found no decreases in subcortical CBF or volume in cART-treated chronically HIV-infected children presenting with substantially poorer cognitive functioning and widespread MRI abnormalities as compared to healthy controls. These results do not provide support for the biphasic disease pattern and suggest that cerebral injury follows a different course in the developing brain of perinatally HIV-infected, cART-treated children.

**Table 3**

**Associations between CBF and HIV disease and treatment characteristics.**

| HIV disease and treatment characteristics | N | Gray matter CBF | | White matter CBF | | Caudate nucleus CBF | | Putamen CBF | | Nucleus accumbens CBF | | Thalamus CBF | |
|---|---|---|---|---|---|---|---|---|---|---|---|---|---|
| | | Coef. | P | Coef. | P | Coef. | P | Coef. | P | Coef. | P | Coef. | P |
| CDC diagnosis | | | | | | | | | | | | | |
| CDC stage B | 28 | −1.557 | 0.734 | 0.288 | 0.849 | −0.942 | 0.735 | −1.065 | 0.561 | −0.814 | 0.689 | 6.451 | 0.005** |
| CDC stage C | 28 | 0.119 | 0.982 | −0.040 | 0.981 | −1.183 | 0.704 | −0.404 | 0.843 | 1.385 | 0.545 | 8.518 | 0.001** |
| Viral load | | | | | | | | | | | | | |
| Zenith VL, log copies/mL | 25 | 7.614 | 0.025* | 2.070 | 0.073 | −2.229 | 0.302 | −2.656 | 0.041* | −1.535 | 0.354 | 1.411 | 0.470 |
| Duration of undetectable VL, y | 28 | 0.739 | 0.132 | 0.106 | 0.521 | −0.167 | 0.582 | −0.510 | 0.009** | −0.382 | 0.082 | 0.149 | 0.616 |
| Undetectable blood VL | 28 | 4.247 | 0.492 | 1.551 | 0.445 | −3.736 | 0.315 | −2.167 | 0.379 | −4.151 | 0.129 | 4.727 | 0.192 |
| Undetectable CSF VL | 19 | 5.026 | 0.498 | 4.241 | 0.085 | −0.662 | 0.889 | −2.749 | 0.356 | −3.761 | 0.225 | 7.346 | 0.098 |
| CD4 T-cells | | | | | | | | | | | | | |
| Nadir $CD4^+$ T-cell count (Z-score) | 26 | 1.622 | 0.560 | 0.302 | 0.753 | 2.907 | 0.087 | 1.470 | 0.168 | 1.537 | 0.234 | −1.196 | 0.440 |
| Lifetime duration $CD4^+$ T-cell count $<500 \times 10^6$/L, log mo | 13 | −3.580 | 0.615 | −1.589 | 0.513 | −10.060 | 0.027* | −2.582 | 0.171 | −1.496 | 0.315 | −2.495 | 0.575 |
| $CD4^+$ T-cell count at inclusion (Z-score) | 28 | 3.500 | 0.329 | 0.657 | 0.581 | 2.417 | 0.264 | 2.023 | 0.153 | 0.852 | 0.602 | −0.094 | 0.965 |
| cART | | | | | | | | | | | | | |
| Age at cART initiation, y | 26 | −1.112 | 0.054 | −0.187 | 0.361 | −0.106 | 0.780 | 0.133 | 0.571 | 0.003 | 0.992 | −0.394 | 0.234 |
| cART use at study inclusion | 28 | 4.247 | 0.492 | 1.551 | 0.445 | −3.736 | 0.315 | −2.167 | 0.379 | −4.151 | 0.129 | 4.727 | 0.192 |
| Duration without cART, y | 26 | −0.943 | 0.081 | −0.229 | 0.226 | 0.058 | 0.869 | 0.332 | 0.118 | 0.303 | 0.243 | −0.488 | 0.107 |

Results of the age, sex, and hematocrit (Ht)-adjusted linear regression analysis exploring potential associations between CBF (mL/100 g/min) and HIV disease and treatment characteristics. CBF was calculated with corrections for the effect of Ht on blood T1 and for partial volume fractions. Subcortical CBF values were normalized subject-wise using the overall mean gray matter CBF. Variables with a skewed distribution (zenith HIV viral load, duration of CD4 T-cell count $<500 \times 10^6$/L) were transformed using base 10 log to approach a normal distribution. Nadir and current CD4 T-cell counts were transformed to age-specific Z-scores.

B = moderate symptoms, C = severe symptoms or acquired immunodeficiency syndrome, cART = combination antiretroviral therapy, CBF = cerebral blood flow, CDC stage = Center for Disease Control and Prevention stage, CSF = cerebrospinal fluid, HIV = human immunodeficiency virus, N/A = no/minimal symptoms [reference category], nadir CD4 = lowest CD4 T-cell count, VL = viral load, zenith VL = highest viral load, Z-score = age-specific normalized score.

* $P < 0.05$.

** $P < 0.01$.

**Table 4**

**Gray matter CBF is associated with white matter lesion volume in HIV-infected children.**

| | Gray matter volume†, $cm^3$ | | White matter volume†, $cm^3$ | | Caudate nucleus volume†, $cm^3$ | | Putamen volume†, $cm^3$ | | Nucleus accumbens volume†, $cm^3$ | | Thalamus volume†, $cm^3$ | | WML prevalence‡ | | WML volume§, log $mm^3$ | |
|---|---|---|---|---|---|---|---|---|---|---|---|---|---|---|---|---|
| | Coef. | *P* | Coef. | *P* | Coef. | *P* | Coef. | *P* | Coef. | *P* | Coef. | *P* | Coef. | *P* | Coef. | *P* |
| HIV-infected | | | | | | | | | | | | | | | | |
| Gray matter CBF | −0.133 | 0.869 | 0.467 | 0.563 | −0.002 | 0.931 | −0.010 | 0.712 | 0.006 | 0.192 | −0.027 | 0.319 | −0.261 | 0.054 | −0.053 | 0.039* |
| White matter CBF | — | | −1.469 | 0.567 | — | | — | | — | | — | | −0.123 | 0.431 | −0.017 | 0.852 |
| Caudate nucleus CBF | — | | — | | 0.099 | 0.175 | — | | — | | — | | — | | — | |
| Putamen CBF | — | | — | | — | | 0.026 | 0.696 | — | | — | | — | | — | |
| Nucleus accumbens CBF | — | | — | | — | | — | | −0.028 | 0.597 | — | | — | | — | |
| Thalamus CBF | — | | — | | — | | — | | — | | 0.012 | 0.169 | — | | — | |
| Healthy controls | | | | | | | | | | | | | | | | |
| Gray matter CBF | 2.037 | 0.085 | 0.640 | 0.351 | 0.019 | 0.335 | 0.028 | 0.287 | 0.006 | 0.237 | 0.042 | 0.143 | 0.017 | 0.786 | −0.002 | 0.924 |
| White matter CBF | — | | 0.171 | 0.950 | — | | — | | — | | — | | 0.115 | 0.629 | 0.029 | 0.650 |
| Caudate nucleus CBF | — | | — | | 0.091 | 0.012* | — | | — | | — | | — | | — | |
| Putamen CBF | — | | — | | — | | 0.054 | 0.248 | — | | — | | — | | — | |
| Nucleus accumbens CBF | — | | — | | — | | — | | 0.007 | 0.221 | — | | — | | — | |
| Thalamus CBF | — | | — | | — | | — | | — | | −0.089 | 0.071 | — | | — | |

Results of the linear regression analysis exploring associations between CBF (mL/100 g/min) and macrostructural MRI biomarkers.[2] CBF was calculated with corrections for the effect of hematocrit (Ht) on blood T1 and for partial volume fractions. Subcortical CBF values were normalized subject-wise using the overall mean gray matter CBF. All analyses were adjusted for age, sex, Ht, and additionally for intracranial volume in case of volumetric outcomes.

CBF = cerebral blood flow, HIV = human immunodeficiency virus, MRI = magnetic resonance imaging, WML = white matter lesion.

† HIV-infected: N = 26; controls: N = 34.

‡ HIV-infected: N = 25; controls: N = 32.

§ HIV-infected: N = 24; controls: N = 32.

* $P < 0.05$.

**Table 5**

**CBF is not associated with HIV-related microstructural injury.**

| WM diffusivity | Fractional anisotropy | | Mean diffusivity | | Radial diffusivity | | Axial diffusivity | |
|---|---|---|---|---|---|---|---|---|
| | Coef. | P | Coef. | P | Coef. | P | Coef. | P |
| HIV-infected (n = 28) | | | | | | | | |
| GM CBF | 0.007 | 0.900 | 0.011 | 0.816 | −0.001 | 0.992 | 0.036 | 0.553 |
| WM CBF | −0.095 | 0.604 | 0.195 | 0.196 | 0.189 | 0.340 | 0.206 | 0.264 |
| Healthy controls (n = 34) | | | | | | | | |
| GM CBF | 0.043 | 0.313 | 0.035 | 0.336 | 0.002 | 0.970 | 0.100 | 0.015* |
| WM CBF | 0.181 | 0.308 | 0.015 | 0.921 | −0.091 | 0.637 | 0.226 | 0.199 |
| **WM neurometabolites** | **NAA:Cre** | | **Glu:Cre** | | **mI:Cre** | | **Cho:Cre** | |
| | Coef. | P | Coef. | P | Coef. | P | Coef. | P |
| HIV-infected (n = 24) | | | | | | | | |
| GM CBF | −0.0002 | 0.947 | −0.0041 | 0.132 | −0.0012 | 0.405 | −0.0002 | 0.761 |
| WM CBF | −0.0027 | 0.720 | −0.0091 | 0.307 | −0.0079 | 0.075 | −0.0016 | 0.536 |
| Healthy controls (n = 33) | | | | | | | | |
| GM CBF | 0.0024 | 0.252 | 0.0033 | 0.195 | 0.0006 | 0.581 | 0.0000 | 0.995 |
| WM CBF | 0.0069 | 0.423 | 0.0020 | 0.850 | 0.0008 | 0.849 | −0.0006 | 0.792 |
| **GM neurometabolites** | **NAA:Cre** | | **Glu:Cre** | | **mI:Cre** | | **Cho:Cre** | |
| | Coef. | P | Coef. | P | Coef. | P | Coef. | P |
| HIV-infected (n = 24) | | | | | | | | |
| GM CBF | −0.0005 | 0.820 | −0.0017 | 0.527 | 0.0012 | 0.362 | −0.0003 | 0.619 |
| Healthy controls (n = 33) | | | | | | | | |
| GM CBF | 0.0002 | 0.924 | 0.0046 | 0.055 | 0.0007 | 0.416 | 0.00004 | 0.926 |

Results of the linear regression analysis exploring associations between CBF (mL/100 g/min) and WM diffusivity as measured with diffusion tensor imaging,[2] and with neurometabolites as measured with magnetic resonance spectroscopy.[5] CBF was calculated with corrections for the effect of hematocrit (Ht) on blood T1 and for partial volume fractions. Subcortical CBF values were normalized subject-wise using the overall mean GM CBF. All analyses were adjusted for age, sex, and Ht.

CBF = cerebral blood flow, Cho = choline, Cre = creatine, Glu = glutamate, GM = gray matter, HIV = human immunodeficiency virus, mI = myo-inositol, NAA = N-acetylaspartate, WM = white matter.

* $P < 0.05$.

In the present study, thalamic flow was highest in children with a CDC B or C diagnosis, while a longer period of viral suppression was associated with lower caudate flow. This suggests that some of the CBF changes found in our cohort of cART-treated children may reflect cerebral injury sustained during unsuppressed HIV infection. Perinatal HIV-infection may indeed cause damage to the brain very early in life, as the virus has been shown to enter the CNS within days of infection.[31] Further, WML have been detected in perinatally HIV-infected children who were started on cART as early as 8 weeks after birth.[3] Several recent neuroimaging studies in cART-treated children and adolescents have also shown associations between MRI abnormalities and early life HIV disease severity.[2,5,32] These studies imply that cerebral injury is at least partly acquired during early unsuppressed HIV infection, and is not fully recovered after initiation of treatment. Contrastingly, higher zenith HIV VL and

**Table 6**

**CBF is not associated with cognitive impairment in HIV-infected children.**

| | IQ | | Processing speed | | Attention/working memory | | Visuomotor integration | |
|---|---|---|---|---|---|---|---|---|
| | Coef. | P | Coef. | P | Coef. | P | Coef. | P |
| HIV-infected (n = 28) | | | | | | | | |
| GM CBF | −0.040 | 0.882 | 0.165 | 0.417 | −0.071 | 0.279 | 0.285 | 0.754 |
| WM CBF | −0.545 | 0.515 | −0.159 | 0.804 | −0.258 | 0.203 | 0.499 | 0.078 |
| Caudate nucleus CBF | −0.101 | 0.891 | −0.409 | 0.462 | 0.206 | 0.247 | −0.225 | 0.778 |
| Putamen CBF | −0.756 | 0.237 | −0.399 | 0.415 | −0.045 | 0.776 | −0.507 | 0.468 |
| Nucleus accumbens CBF | −0.833 | 0.093 | −0.268 | 0.488 | −0.070 | 0.576 | 0.385 | 0.484 |
| Thalamus CBF | −0.691 | 0.146 | −0.565 | 0.116 | −0.085 | 0.476 | −0.844 | 0.099 |
| Healthy controls (n = 34) | | | | | | | | |
| GM CBF | 0.236 | 0.365 | 0.287 | 0.127 | 0.107 | 0.029* | 0.071 | 0.940 |
| WM CBF | −0.502 | 0.644 | 0.376 | 0.637 | 0.201 | 0.338 | 0.131 | 0.565 |
| Caudate nucleus CBF | −0.394 | 0.460 | 0.263 | 0.502 | −0.073 | 0.479 | −0.194 | 0.679 |
| Putamen CBF | −0.312 | 0.518 | 0.151 | 0.671 | −0.084 | 0.367 | −0.153 | 0.717 |
| Nucleus accumbens CBF | 0.088 | 0.854 | 0.639 | 0.061 | −0.019 | 0.840 | −0.060 | 0.885 |
| Thalamus CBF | 0.146 | 0.632 | −0.047 | 0.834 | −0.002 | 0.969 | 0.223 | 0.399 |

Results of the linear regression analysis exploring associations between CBF (mL/100 g/min) and cognitive performance.[13] CBF was calculated with corrections for the effect of hematocrit (Ht) on blood T1 and for partial volume fractions. Subcortical CBF values were normalized subject-wise using the overall mean gray matter CBF. All analyses were adjusted for age, sex, and Ht.

CBF = cerebral blood flow, GM = gray matter, HIV = human immunodeficiency virus, IQ = intelligence quotient, WM = white matter.

* $P < 0.05$.

a longer duration of immune deficiency ($CD4^+$ T-cell count $<500 \times 10^6$/L) were associated with lower regional CBF. These findings do not support the theory that CBF changes are largely caused by injury sustained during unsuppressed HIV-infection, and imply that other factors may have been at play. The exact interplay between early life HIV-related factors and CBF should thus be evaluated in multivariable models in larger study samples. There were no associations between CBF and HIV disease or treatment factors at study inclusion, likely because most patients in our cohort had achieved optimal virological suppression and immune reconstitution with adequate cART treatment at that time. These findings allude to a protective effect of cART, but strongly suggest that for optimal development of the brain in perinatally HIV-infected children, the window to initiate treatment may be narrow.

In contrast with earlier studies in children[8] and adults,[21,33] we did not find lower GM CBF in HIV-infected children as compared to controls. However, HIV-infected children with lower GM CBF had a higher volume of WML. This could imply that the observed WML are—at least in part—caused by subtle or fluctuating alterations in GM CBF, which could lead to ischemia in adjacent WM, especially in watershed areas.[34] This theory is consistent with early signs of atherosclerosis (i.e., increased carotid media thickness and reduced flow-mediated distension[35]) in HIV-infected children, which are known risk factors for hemodynamic insufficiency-related WM injury in adults.[36] However, WML in HIV-infected children are not confined to periventricular watershed areas,[2,3] and these lesions may thus not be exclusively caused by large-vessel mediated hemodynamic insufficiency. While WM CBF was not associated with WML, this does not rule out localized WM CBF deficits as seen in small vessel pathology, which may contribute to WML formation without exerting a detectable influence on whole brain WM CBF.[34]

The overall higher WM CBF detected in HIV-infected children could reflect a slight increase in local metabolic activity, such as glial proliferation, neuroinflammation, or compensation for injury. A study focusing on patients with MS, a disorder characterized by CNS inflammation and macro- and microstructural WM injury, reported higher CBF in normal appearing WM in association with increased inflammatory activity in the brain.[37] Higher WM CBF in HIV-infected children may similarly indicate ongoing neuroinflammation in the setting of chronic infection. Indeed, several studies in HIV-infected children report findings that are suggestive of ongoing systemic and intrathecal inflammation and immune activation despite cART, including increased levels of pro-inflammatory mediators,[38] monocyte activation markers,[39] and vascular endothelial activation molecules.[40] Further, we previously detected a higher choline-to-creatine neurometabolite ratio in HIV-infected children, another potential marker of cerebral inflammation.[5] These findings are consistent with neuropathology reports of WM gliosis and inflammatory lesions in HIV-infected children.[41] Higher WM CBF could also be a physiological response to deliver more oxygen to the brain following lower Ht, as was proposed in children with sickle cell anemia.[42] This mechanism is, however, unlikely to explain the findings in our cohort, as our adjustments for Ht should have largely attenuated Ht-driven CBF differences between groups.

In healthy controls, higher GM CBF was associated with better axonal integrity, as indicated by higher AD, and with better attention and working memory performance. This is in line with other studies in healthy children that report a positive correlation between cognitive functioning and GM CBF.[10,43] We did not detect any associations between CBF and poorer cognitive functioning in HIV-infected children. Resting state CBF may thus not be a reliable marker for HIV-related cognitive impairment in the pediatric population, but this should be confirmed in larger studies.

Our study is the first to evaluate ASL-measured CBF in cART-treated HIV-infected children, but the observed changes were subtle and our sample relatively small. This may have hampered the detection of potential correlations between CBF changes and other indicators of HIV-induced cerebral injury and cognitive dysfunction. The cross-sectional nature of our study does not allow to differentiate the cause from effect, which limits interpretations concerning the pathogenesis of CBF alterations in pediatric HIV. Additionally, as most HIV-infected children in our cohort have been treated with cART for the majority of their life, separate effects of HIV infection and cART cannot be distinguished in this study. We did, however, exclusively detect correlations between CBF and HIV-related variables, but none with cART-related variables, suggesting that cART does not (further) alter CBF in HIV-infected children. We measured CBF in resting state and not during task-based activation, which limits relating CBF to functioning or impairments in specific neurocognitive domains. Lastly, in accordance with the exploratory nature of the study, we performed multiple comparisons without further correction, and results should be interpreted accordingly.

## 5. Conclusion

The present study shows that subcortical and WM CBF are higher in cART-treated HIV-infected children as compared to healthy controls. The differences were subtle, and CBF in these regions was not directly associated with HIV-related cerebral injury or cognitive impairment. Nonetheless, the association between lower GM CBF and higher WML volume in HIV-infected children could imply that poorer vascular health may contribute to WM injury over time. These findings could improve our understanding of the pathogenesis of cerebral injury and should be further studied.

To identify the mechanisms underlying CBF changes and understand how they relate to WML in HIV-infected children, relationships between CBF and markers of inflammation, vascular endothelial activation, coagulation, and neurodegeneration should be further explored. Finally, lifelong exposure to HIV and cART, with concomitant increased risks of neurocognitive and vascular dysfunction, warrant longitudinal monitoring of this population to observe how CBF and cerebral changes evolve over time.

## Acknowledgments

The authors thank to all study participants, to A.W. Weijsenfeld and A. van der Plas for recruiting patients, to Drs. J.A. ter Stege for performing neuropsychological assessments, to Dr. P.W. Hales for contributing the calculation model for the effect of Ht on the T1 relaxation time of blood, and to Dr. A. Leemans for his work on the ExploreASL toolbox.

## References

[1] Blokhuis C, Kootstra NA, Caan MW, et al. Neurodevelopmental delay in pediatric HIV/AIDS: current perspectives. Neurobehav HIV Med 2016;7:1–3.

[2] Cohen S, Caan MWA, Mutsaerts HJ, et al. Cerebral injury in perinatally HIV-infected children compared to matched healthy controls. Neurology 2016;86:19–27.

[3] Ackermann C, Andronikou S, Laughton B, et al. White matter signal abnormalities in children with suspected HIV-related neurologic disease on early combination antiretroviral therapy. Pediatr Infect Dis J 2014;33: e207–12.
[4] Hoare J, Fouche J-P, Spottiswoode B, et al. A diffusion tensor imaging and neurocognitive study of HIV-positive children who are HAART-naïve "slow progressors". J Neurovirol 2012;18:205–12.
[5] Van Dalen YW, Blokhuis C, Cohen S, et al. Neurometabolite alterations associated with cognitive performance in perinatally HIV-infected children. Medicine 2016;95:e3093.
[6] Hammond CK, Eley B, Wieselthaler N, et al. Cerebrovascular disease in children with HIV-1 infection. Dev Med Child Neurol 2016;58:452–60.
[7] Barlow-Mosha L, Eckard AR, McComsey GA, et al. Metabolic complications and treatment of perinatally HIV-infected children and adolescents. J Int AIDS Soc 2013;16:18600.
[8] Depas G, Chiron C, Tardieu M, et al. Functional brain imaging in HIV-1-infected children born to seropositive mothers. J Nucl Med 1995;36: 2169–74.
[9] Proisy M, Bruneau B, Rozel C, et al. Arterial spin labeling in clinical pediatric imaging. Diagn Interv Imaging 2015;97:151–8.
[10] Kilroy E, Liu CY, Yan L, et al. Relationships between cerebral blood flow and IQ in typically developing children and adolescents. J Cogn Sci (Seoul) 2011;12:151–70.
[11] Strouse JJ, Cox CS, Melhem ER, et al. Inverse correlation between cerebral blood flow measured by continuous arterial spin-labeling (CASL) MRI and neurocognitive function in children with sickle cell anemia (SCA). Blood 2006;108:379–81.
[12] Ances BM, Roc AC, Wang J, et al. Caudate blood flow and volume are reduced in HIV+ neurocognitively impaired patients. Neurology 2006; 66:862–6.
[13] Cohen S, Stege JA, Geurtsen GJ, et al. Poorer cognitive performance in perinatally HIV-infected children versus healthy socioeconomically matched controls. Clin Infect Dis 2015;60:1111–9.
[14] Puthanakit T, Ananworanich J, Vonthanak S, et al. Cognitive function and neurodevelopmental outcomes in HIV-infected children older than 1 year of age randomized to early versus deferred antiretroviral therapy: the PREDICT neurodevelopmental study. Pediatr Infect Dis J 2013;32: 501–8.
[15] Fischl B, Salat DH, Busa E, et al. Whole brain segmentation: automated labeling of neuroanatomical structures in the human brain. Neuron 2002;33:341–55.
[16] Mutsaerts H, Thomas D, Petr J, et al. Addressing multi-centre image registration of 3T arterial spin labeling images from the GENetic Frontotemporal dementia Initiative (GENFI). Paper presented at: the ISMRM 24th Annual Meeting and Exhibition, May 7–13, 2016; Singapore.
[17] Wang Z, Aguirre GK, Rao H, et al. Empirical optimization of ASL data analysis using an ASL data processing toolbox: ASLtbx. Magn Reson Imaging 2008;26:261–9.
[18] Lemieux L, Salek-Haddadi A, Lund TE, et al. Modelling large motion events in fMRI studies of patients with epilepsy. Magn Reson Imaging 2007;25:894–901.
[19] Alsop DC, Detre JA, Golay X, et al. Recommended implementation of arterial spin-labeled perfusion MRI for clinical applications: a consensus of the ISMRM Perfusion Study group and the European consortium for ASL in dementia. Magn Reson Med 2015;73:102–16.
[20] Hales PW, Kirkham FJ, Clark CA. A general model to calculate the spin-lattice (T1) relaxation time of blood, accounting for haematocrit, oxygen saturation and magnetic field strength. J Cereb Blood Flow Metab 2015; 36:370–4.
[21] Ances BM, Sisti D, Vaida F, et al. Resting cerebral blood flow: a potential biomarker of the effects of HIV in the brain. Neurology 2009;73:702–8.
[22] Towgood KJ, Pitkanen M, Kulasegaram R, et al. Regional cerebral blood flow and FDG uptake in asymptomatic HIV-1 men. Hum Brain Mapp 2013;34:2484–93.
[23] Ashburner J, Friston KJ. Voxel-based morphometry—the methods. Neuroimage 2000;11:805–21.
[24] Mutsaerts HJMM, Richard E, Heijtel DFR, et al. Gray matter contamination in arterial spin labeling white matter perfusion measurements in patients with dementia. Neuroimage Clin 2014;4:139–44.
[25] Desikan RS, Ségonne F, Fischl B, et al. An automated labeling system for subdividing the human cerebral cortex on MRI scans into gyral based regions of interest. Neuroimage 2006;31:968–80.
[26] Asllani I, Borogovac A, Brown TR. Regression algorithm correcting for partial volume effects in arterial spin labeling MRI. Magn Reson Med 2008;60:1362–71.
[27] Biagi L, Abbruzzese A, Bianchi MC, et al. Age dependence of cerebral perfusion assessed by magnetic resonance continuous arterial spin labeling. J Magn Reson Imaging 2007;25:696–702.
[28] van der Veen PH, Muller M, Vincken KL, et al. Hemoglobin, hematocrit, and changes in cerebral blood flow: the Second Manifestations of ARTerial disease-Magnetic Resonance study. Neurobiol Aging 2015;36: 1417–23.
[29] Wenserski F, von Giesen H-J, Wittsack H-J, et al. Human immunodeficiency virus 1-associated minor motor disorders: perfusion-weighted MR imaging and H MR spectroscopy. Radiology 2003;228:185–92.
[30] Meyerhoff DJ, Bloomer C, Cardenas V, et al. Elevated subcortical choline metabolites in cognitively and clinically asymptomatic HIV+ patients. Neurology 1999;52:995–1003.
[31] Valcour V, Chalermchai T, Sailasuta N, et al. Central nervous system viral invasion and inflammation during acute HIV infection. J Infect Dis 2012;206:275–82.
[32] Uban KA, Herting MM, Williams PL, et al. White matter microstructure among youth with perinatally acquired HIV is associated with disease severity. AIDS 2015;29:1035–44.
[33] Dunlop O, Rootwelt K, Rklund R, et al. Reduced global cerebral blood flow in non-demented HIV positive patients. J NeuroAIDS 1996;1: 71–8.
[34] Promjunyakul N, Lahna D, Kaye JA, et al. Characterizing the white matter hyperintensity penumbra with cerebral blood flow measures. Neuroimage Clin 2015;8:224–9.
[35] Charakida M, Donald AE, Green H, et al. Early structural and functional changes of the vasculature in HIV-infected children: impact of disease and antiretroviral therapy. Circulation 2005;112:103–9.
[36] Kim KW, MacFall JR, Payne ME. Classification of white matter lesions on magnetic resonance imaging in elderly persons. Biol Psychiatry 2008; 64:273–80.
[37] Bester M, Forkert ND, Stellmann JP, et al. Increased perfusion in normal appearing white matter in high inflammatory multiple sclerosis patients. PLoS ONE 2015;10:e0119356.
[38] McCoig C, Castrejón MM, Saavedra-Lozano J, et al. Cerebrospinal fluid and plasma concentrations of proinflammatory mediators in human immunodeficiency virus-infected children. Pediatr Infect Dis J 2004;23: 114–8.
[39] Sainz T, Diaz L, Navarro ML, et al. Cardiovascular biomarkers in vertically HIV-infected children without metabolic abnormalities. Atherosclerosis 2014;233:410–4.
[40] Miller TL, Borkowsky W, Dimeglio LA, et al. Metabolic abnormalities and viral replication are associated with biomarkers of vascular dysfunction in HIV-infected children. HIV Med 2012;13:264–75.
[41] Kure K, Llena JF, Lyman WD, et al. Human immunodeficiency virus-1 infection of the nervous system: an autopsy study of 268 adult, pediatric, and fetal brains. Hum Pathol 1991;22:700–10.
[42] Helton KJ, Paydar A, Glass J, et al. Arterial spin-labeled perfusion combined with segmentation techniques to evaluate cerebral blood flow in white and gray matter of children with sickle cell anemia. Pediatr Blood Cancer 2009;52:85–91.
[43] Bakker MJ, Hofmann J, Churches OF, et al. Cerebrovascular function and cognition in childhood: a systematic review of transcranial Doppler studies. BMC Neurol 2014;14:43.